

Polarimetric heterodyning fiber laser sensor for directional acoustic signal measurement

Chengang Lyu,^{1,*} Chuang Wu,^{3,4} Hwa-Yaw Tam,³ Chao Lu,² and Jianguo Ma¹

¹ School of Electronic Information Engineering, Tianjin University, Tianjin 300072, China

² Photonics Research Center, Department of Electronic and Information Engineering, The Hong Kong Polytechnic University, Kowloon, Hong Kong SAR, China

³ Photonics Research Centre, Department of Electrical Engineering, The Hong Kong Polytechnic University, Kowloon, Hong Kong SAR, China

⁴ Institute of Photonics Technology, Jinan University, Guangzhou 510632, China

*lvchengang@tju.edu.cn

Abstract: A DBR fiber grating laser acoustic sensor based on polarization beat signal modulation analysis has been demonstrated for directional acoustic signal measurement. The acoustic sensor was fabricated in birefringent erbium-doped fiber, and the influences of external-acoustic pressure on fiber grating laser sensor were analyzed, considering the effect of relative orientation of the acoustic wave on the degrees of birefringence modulation. In experiment, the birefringence in sensing fiber was modulated by ultrasonic pressure. Agreement between theoretical and experimental results was obtained for ultrasound wave propagating from different directions (0-360 degrees in 15 degrees intervals) corresponding to a nonlinearly change in beat frequency modulation rates. The results demonstrate that the DBR fiber grating laser acoustic sensor has an orientation recognizable ability, offering a potential for acoustic vector signal detection.

©2013 Optical Society of America

OCIS codes: (060.2370) Fiber optics sensors; (060.3510) Lasers; (060.2840) Heterodyne.

References and links

1. B. Dunmire, K. W. Beach, K. H. Labs, M. Plett, and D. E. Strandness, Jr., "Cross-beam vector Doppler ultrasound for angle-independent velocity measurements," *Ultrasound Med. Biol.* **26**(8), 1213–1235 (2000).
2. T. Harrison, J. C. Ranasinghesagara, H. Lu, K. Mathewson, A. Walsh, and R. J. Zemp, "Combined photoacoustic and ultrasound biomicroscopy," *Opt. Express* **17**(24), 22041–22046 (2009).
3. H. Sielschott, "Measurement of horizontal flow in a large scale furnace using acoustic vector tomography," *Flow Meas. Instrum.* **8**(3–4), 191–197 (1997).
4. Y. I. Wu, K. T. Wong, and S.-K. Lau, "The acoustic vector-sensor's near-field array-manifold," *IEEE T. Signal Process.* **58**(7), 3946–3951 (2010).
5. G. A. Miller, G. A. Cranch, and C. K. Kirkendall, "High-Performance Sensing Using Fiber Lasers," *Opt. Photon. News* **23**(2), 30–36 (2012).
6. B. Culshaw and A. Kersey, "Fiber-Optic Sensing: A Historical Perspective," *J. Lightwave Technol.* **26**(9), 1064–1078 (2008).
7. W. Wang, N. Wu, Y. Tian, X. Wang, C. Niezrecki, and J. Chen, "Optical pressure/acoustic sensor with precise Fabry-Perot cavity length control using angle polished fiber," *Opt. Express* **17**(19), 16613–16618 (2009).
8. M. Moccia, M. Pisco, A. Cutolo, V. Galdi, P. Bevilacqua, and A. Cusano, "Opto-acoustic behavior of coated fiber Bragg gratings," *Opt. Express* **19**(20), 18842–18860 (2011).
9. R. Guan, F. Zhu, Z. Gan, D. Huang, and S. Liu, "Stress birefringence analysis of polarization maintaining optical fibers," *Opt. Fiber Technol.* **11**(3), 240–254 (2005).
10. M. Karimi, F. Surre, T. Sun, K. T. V. Grattan, W. Margulis, and P. Fojallaz, "Directional force measurement using specialized single-mode polarization-maintaining fibers," *J. Lightwave Technol.* **29**(24), 3611–3615 (2011).
11. H. K. Kim, S. K. Kim, H. G. Park, and B. Y. Kim, "Polarimetric fiber laser sensors," *Opt. Lett.* **18**(4), 317–319 (1993).
12. H. K. Kim, S. K. Kim, and B. Y. Kim, "Polarization control of polarimetric fiber-laser sensors," *Opt. Lett.* **18**(17), 1465–1467 (1993).
13. G. A. Ball, G. Meltz, and W. W. Morey, "Polarimetric heterodyning Bragg-grating fiber-laser sensor," *Opt. Lett.* **18**(22), 1976–1978 (1993).
14. J. T. Kringlebotn, W. H. Loh, and R. I. Laming, "Polarimetric Er³⁺-doped fiber distributed-feedback laser sensor

- for differential pressure and force measurements,” *Opt. Lett.* **21**(22), 1869–1871 (1996).
15. K. Bohnert, A. Frank, E. Rochat, K. Haroud, and H. Brändle, “Polarimetric fiber laser sensor for hydrostatic pressure,” *Appl. Opt.* **43**(1), 41–48 (2004).
 16. A. Frank, K. Haroud, E. Rochat, K. Bohnert, H. Brandle, and Ieee, “High resolution fiber laser sensor for hydrostatic pressure,” in *OFS 2002: 15th Optical Fiber Sensors Conference Technical Digest*(IEEE, New York, 2002), pp. 359–362.
 17. B.-O. Guan, H.-Y. Tam, S.-T. Lau, and H. L. W. Chan, “Ultrasonic hydrophone based on distributed Bragg reflector fiber laser,” *IEEE. Photon. Technol. Lett.* **17**(1), 169–171 (2005).
 18. H. Y. Tam, H. L. W. Chan, and B. O. Guan, “Ultrasound sensor and ultrasound measurement device,” U.S. Patent 7206259 B2 (Apr. 2007).
 19. B.-O. Guan, L. Jin, Y. Zhang, and H.-Y. Tam, “Polarimetric heterodyning fiber grating laser sensors,” *J. Lightwave Technol.* **30**(8), 1097–1112 (2012).

1. Introduction

Acoustic sensor has been extensively applied to the applications in ultrasound clinic imaging, crack detections of buildings, etc [1–3]. The required information can be obtained by measuring the frequencies, power densities and propagation directions of the acoustic waves used basically [4]. Fiber optic sensors offer many advantages over acoustic sensors including small size, immunity from EMI, and absence of electrical components [5,6]. The fiber optic acoustic sensors, which are operated in interferometric techniques [7] and fiber grating techniques [8], can be applied to separately quantify the power density and the frequency of the acoustic wave, but their response to acoustic directional signals is relatively low.

Polarization-sensitive optical fiber can provide the directional informations, which based on birefringence due to the anisotropic in optical fiber core [9,10]. The polarimetric heterodyning fiber laser sensor, first demonstrated by Kim et al. [11,12], was applied to measure the static external perturbations [13–16]. But their reported sensors were not beneficial for the acoustic detection due to the unstable multi-longitudinal-mode beating signal outputs. In recent years, a polarimetric heterodyning distributed-Bragg-reflector (DBR) fiber grating laser sensor with single-longitudinal-mode output was proposed and demonstrated by Tam and Guan et al., showing the attractive advantage on the acoustic frequency and power density sensing [17–19].

In this paper we study the possibility of acoustic signals detection with directivity by means of the DBR fiber grating laser sensor. We carry out theoretical analysis to evaluate the relationship between acoustic directional pressure and modulation of polarization beat signals. Good agreement between theoretical and experimental results was achieved. Experimental results shown that the polarization beat frequency was modulated in varying degrees as a function of angle where the applied external ultrasound transverse pressure on the fiber laser sensor. Over a certain range of frequency and power density of the ultrasound signal, the DBR fiber grating laser acoustic sensor has shown an orientation-recognizable ability.

2. Principle

Figure 1(a) shows the schematic of a DBR fiber laser sensor consisting of a pair of wavelength-matched Bragg gratings written in an Er^{3+} doped fiber with appropriate separation, to form the laser cavity. When the cavity is shorter than 2-3 cm, the resonant mode spacing is close to or longer than the grating reflection bandwidth, the laser will lase with single-longitudinal mode as shown in Fig. 1(b).

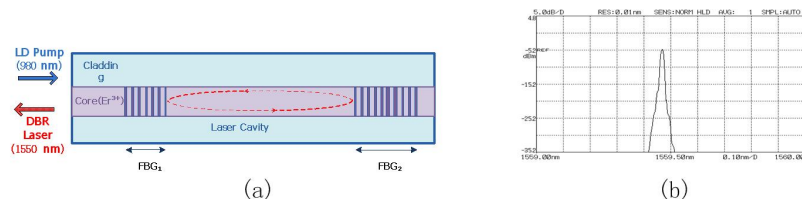


Fig. 1. (a) Schematic of the DBR fiber laser sensor. (b) Output spectrum of the DBR fiber laser

The single-mode active fiber is in fact bimodal, and supports two nearly degenerate orthogonal polarizations of LP_{01x} and LP_{01y} mode. The frequency difference $\Delta\nu$ between the two modes is given by:

$$\Delta\nu = \nu_x - \nu_y = \frac{c}{n_0\lambda_0} B. \quad (1)$$

Where n_0 is the average index of the fiber, λ_0 is the Bragg wavelength of the fiber grating, and $B = n_x - n_y$ is the modal birefringence. Equation (1) suggests that when a DBR fiber laser sensor is placed in an acoustic field, the variations of modal birefringence $\delta n_{x,y}$ (or $\delta\epsilon_{x,y}$, where ϵ is dielectric constant) would result in a change of beat frequency.

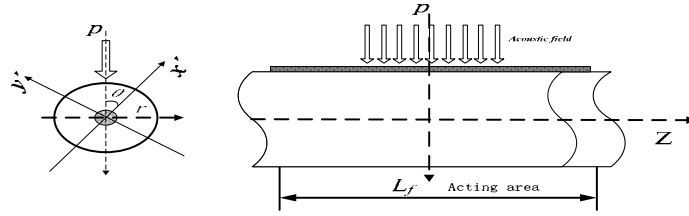


Fig. 2. The acoustic pressure P applied on the fiber cavity at an angle θ to the x' axis

Therefore when the DBR fiber laser sensor is subjected to an acoustic field, and positioned in a direction perpendicular to the surface modulated by acoustic pressure, shown in Fig. 2, the acoustic pressure breaks the near degeneracy by causing an unequal variation in the phase velocity of each eigenmode. The electric field of the fiber laser output measured by a photodetector and RF spectrum analyzer can be represented as follows:

$$E_i = E_b \cos[\omega_b t + \phi(t)]. \quad (2)$$

Where ω_b is frequency of the beat signal, $\phi(t)$ is instantaneous phase deviation induced by the acoustic pressure, and the instantaneous frequency change of the beating signal is defined as:

$$\delta(t) = U_u \cos(\omega_u t + \psi_0). \quad (3)$$

Where U_u , ω_u and ψ_0 are the amplitude, frequency and phase constant of the acoustic wave. So the observed light field modulated by acoustic wave can also be represented as:

$$\begin{aligned} E_i &= E_b \cos[\omega_b t + k_f \int_{-\infty}^t \delta(t) dt] = E_b \cos[\omega_b t + k_f \int_{-\infty}^t U_u \cos(\omega_u t + \psi_0) dt] \\ &= E_b \cos[\omega_b t + M_f \sin(\omega_u t + \psi_0)]. \end{aligned} \quad (4)$$

Where $M_f = \frac{U_u}{\omega_u} k_f$ is the modulation index, and when the acoustic pressure field is stable (U_u and ω_u are constant), it is only affected by the modulation sensitivity k_f , which can be written as:

$$k_f = K \cdot \delta\epsilon_{xy}. \quad (5)$$

Where K is a constant depending on the parameters of optical fiber, and $\delta\epsilon_{xy}$ is the variations of dielectric constant of each eigenmode. Under the acoustic pressure, $\delta\epsilon_{xy}$ is produced by the strain tensor e' along the x' and y' axes, as defined in Fig. 2.

$$\delta\epsilon_x = -\epsilon^2[(P_{11} \cos^2 \theta + P_{12} \sin^2 \theta)e'_x + (P_{11} \sin^2 \theta + P_{12} \cos^2 \theta)e'_y]. \quad (6)$$

$$\delta\epsilon_y = -\epsilon^2[(P_{11} \sin^2 \theta + P_{12} \cos^2 \theta)e'_x + (P_{11} \cos^2 \theta + P_{12} \sin^2 \theta)e'_y]. \quad (7)$$

$$\delta\epsilon_{xy} = \delta\epsilon_x - \delta\epsilon_y = 2\epsilon^2 P_{44}(e'_y - e'_x) \cos 2\theta. \quad (8)$$

Where ϵ is the dielectric constant of the fiber cladding, P_{11} , P_{12} , $P_{44} = (P_{11} - P_{12})/2$ are the elasto-optic coefficients of the fiber, and θ is the angle between the fast axis of the fiber and propagation direction of the acoustic wave.

According to Eq. (8), the modulation sensitivity is zero theoretically at $\theta = \pi/4 \pm n(\pi/2)$, when the induced dielectric constants along the x' and y' axes are identical. And the modulation sensitivity approaches maximum at $\theta = n(\pi/2)$, where the principal polarization axes of the fiber is aligned with the propagation direction of acoustic wave. (Therefore, there are at most three cases corresponding to the angle between the polarization axis of the fiber and the propagation direction of the acoustic wave).

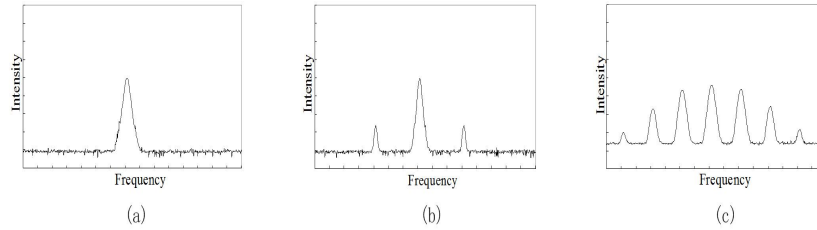


Fig. 3. Acoustic modulation corresponding to different angles between the principal polarization axes of fiber and the propagation direction of acoustic wave. (a) 45°. (b) close to 45°. (c) close to 0° or 90°.

The first case is when the propagation direction of acoustic wave is at 45° with the principal polarization axes of the fiber, we have $k_f = 0$ and Eq. (4) can be written as:

$$E_i = E_b \cos \omega_b t. \quad (9)$$

In this case, the electric field of the DBR laser sensor does not response to acoustic field, as shown in Fig. 3(a).

The second case is when the propagation direction of acoustic wave is close to 45° with the principal polarization axes of fiber, where $\phi(t) < \pi/6$. We have relatively small k_f , and Eq. (4) can be simplified as:

$$\begin{aligned} E_i &\approx E_b(\cos \omega_b t - M_f \sin \omega_b t \cdot \sin \omega_a t) \\ &= E_b[\cos \omega_b t + (M_f/2)\cos(\omega_b + \omega_a)t - (M_f/2)\cos(\omega_b - \omega_a)t]. \end{aligned} \quad (10)$$

In this case, acoustic pressure produces two sidebands on both sides of laser beat frequency, the peak amplitude of sideband is approximate linearly proportional to the intensity of the acoustic pressure by M_f , shown in Fig. 3(b).

The third case is when the propagation direction of acoustic wave closed to the principal polarization axes of fiber, where $\phi(t) > \pi/6$. We have relatively large k_f , and Eq. (4) can be written as:

$$E_t = E_b \cos(\omega_b t + M_f \sin \omega_u t) = E_b \sum_{n=-\infty}^{\infty} J_n(M_f) \cos(\omega_b + n\omega_u)t. \quad (11)$$

In this case, acoustic pressure produces multiple sidebands on both sides of the laser beat frequency, and the peak amplitudes of sidebands are nonlinearly proportional to the intensity of the acoustic pressure, but are given by the Bessel function of the first kind $J_n(M_f)$, as shown in Fig. 3(c).

Equation (9)-(11) indicates that the DBR fiber laser sensor could provide directional acoustic wave detection by analyzing the sidebands of the frequency spectrum, and work as an orientation-recognizable acoustic sensor.

3. Experiment and results

The experimental setup is shown in Fig. 4. The DBR fiber laser was inscribed in a short length of a commercial Er^{3+} -doped fiber (OFS LRL) which has a peak absorption of 20 dB/m at 1530 nm and a mode field diameter of about 5.2 μm . The FBGs were fabricated using phase-mask grating-writing technique with a 193 nm ArF excimer laser. The lengths of the two FBGs are 25 mm with a 30 dB reflectivity and 15 mm with a 22 dB reflectivity, and are separated by a nominal cavity length of 10 mm.

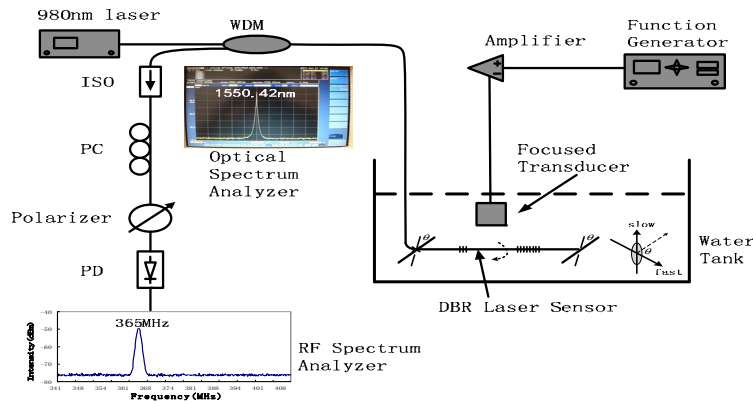


Fig. 4. Experimental setup of the directional acoustic signal measurement based on a short cavity DBR fiber laser sensor. The inset is the photograph of the DBR fiber laser spectrum when it is pumped.

The DBR fiber laser was pumped by a 980 nm laser diode (Bookham LC96X74) with an output power of 450 mW through a 980/1550 nm wavelength division multiplexer (WDM). The 1550.42 nm laser light with the continuous-wave saturation power -9 dBm emitted from the low reflectivity FBG end, and directed to the 1550 nm port of WDM, as shown in Fig. 4. An optical isolator (ISO) was placed in front of the polarization controller (PC) to reduce any unwanted reflection back to the fiber laser. By adjusting the polarization controller (PC) and the polarizer, the two orthogonal polarization lasing modes can be turned to the same polarization state so that strong beating signal of 365 MHz was achieved at the photodetector (PD, Newfocus 1414-FC), shown in the inset of Fig. 4, which is connected to an electrical spectrum analyzer (ESA, Agilent Technologies E8247C).

The DBR fiber laser was fixed on a plastic frame which can be rotated along the fiber's axis, and placed inside a plastic tank filled with water. The plane ultrasound field was generated by an immersion transducer (Panametrics V312) with nominal element size of 6 mm and center frequency of 10 MHz, which was driven in continuous mode. The fiber laser sensor was positioned in the near field of transducer perpendicular to the ultrasound propagation direction.

Figure 5 shows the superimposed beat signal spectra recorded by spectrum analyzer when the acoustic transducer was driven at 8 V with different driving frequency from 8 MHz to 12

MHz. Figure 6 shows the superimposed beat signal spectra when the acoustic transducer was driven at 10 MHz with different driving voltage from 4 V to 10 V. We adjusted and fixed the frame to a proper angle so that the propagation direction of the ultrasonic wave was at close to 45° of the principal polarization axes of fiber, the generated beating signal through the acoustic modulation is as described in the second case of the previous section. As expected from Eq. (10), the peak position of the sideband indicates the frequency of the ultrasound signal, and the peak amplitude of the sideband indicates the ultrasound power density. It can be seen that the amplitude of sideband decreases with the ultrasound frequency in Fig. 5, and increases with the ultrasound power density in Fig. 6. But only in this case of weak modulation, the ultrasound could be analyzed by peak amplitude of the sideband.

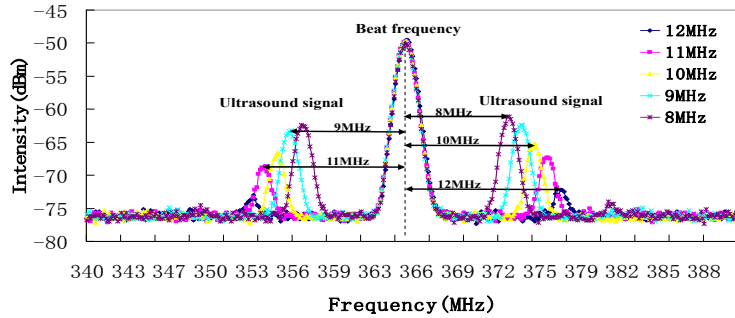


Fig. 5. Modulation spectra when the ultrasound driven at 8 V with different driving frequency

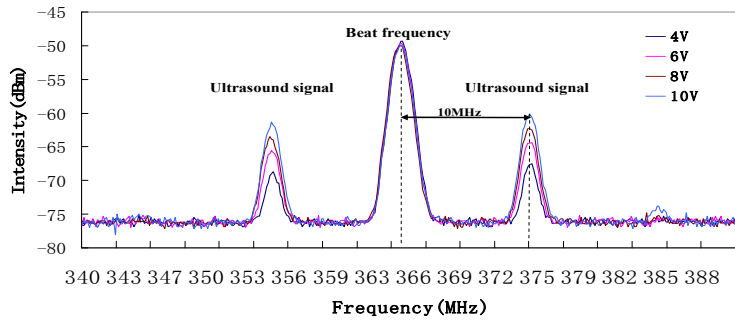


Fig. 6. Modulation spectra when the ultrasound driven at 10 MHz with different driving voltage

When we fixed the driving voltage at 8 V and driving frequency at 8 MHz, by rotating the frame to alter the angle between the propagation direction of the ultrasonic wave and the principal polarization axes of fiber laser sensor, the modulation sensitivity k_f varies from zero to maximum according to Eq. (5), and the modulation process changes according to the cases described above. Figure 7 shows the modulated beat signal spectra when ultrasonic pressure applied to the DBR fiber laser sensor is at various angles θ .

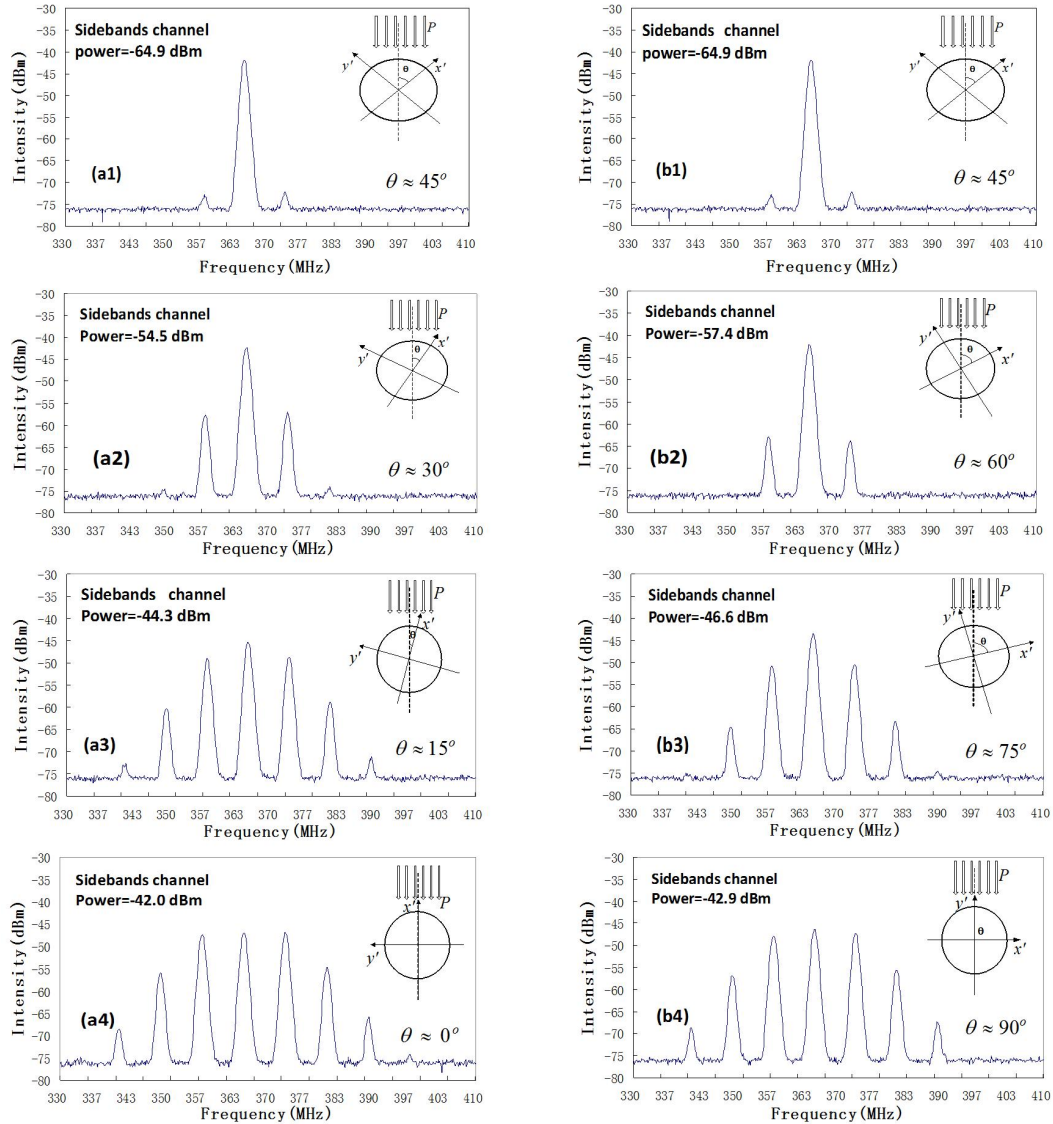


Fig. 7. Modulated beat signal spectra when ultrasonic pressure applied at different angles

When $\theta \approx 45^\circ$, the modulation sensitivity k_f is zero without ultrasonic modulation signals theoretically, and in the experiments due to the adjustment accuracy, the residue signal of sidebands channel power is less than -64 dBm, shown in Figs. 7(a1) and 7(b1). We evaluated the effects of ultrasonic modulation with counterclockwise/clockwise rotation of ultrasound propagation direction in 15 degrees intervals from $\theta \approx 45^\circ$. Figures 7(a2) and 7(b2) shows that first-order sidebands at $f_b \pm 8$ MHz are observed when $\theta \approx 30^\circ$ or $\theta \approx 60^\circ$, and sidebands channel power has increased by around 10 dB within the first 15 degrees regulation. Figures 7(a3) and 7(b3) shows that obvious second-order sidebands at $f_b \pm 16$ MHz are observed when $\theta \approx 15^\circ$ or $\theta \approx 75^\circ$, and sidebands channel power has increased by around 10 dB within the second 15 degrees regulation. Figures 7(a4) and 7(b4) shows that obvious third-order sidebands at $f_b \pm 24$ MHz are observed when $\theta \approx 0^\circ$ or

$\theta \approx 90^\circ$, and sidebands channel power has increased by around 3 dB within the third 15 degrees regulation. Based on Fig. 7, the DBR fiber laser sensor has shown a good ability to detect the acoustic wave direction by sidebands analysis. The results shown that the detection of acoustic propagation direction could be firstly divided into three regions corresponding to the first, second and third-order sidebands, and then in each region signal processing and channel power analysis could be used to quantify the angles of acoustic propagation accurately. Directional patterns of this DBR fiber laser sensor have also been found at acoustic frequency of 8 MHz (0-360 degrees in 15 degrees intervals), shown in Fig. 8. The results demonstrate that the DBR fiber laser acoustic sensor has an orientation-recognizable ability.

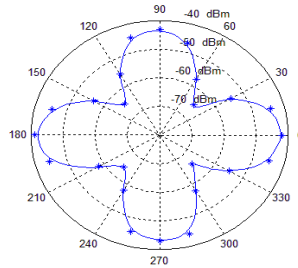


Fig. 8. Directional patterns of DBR fiber laser acoustic sensor

4. Conclusion

The directional characteristics of a polarimetric heterodyning DBR fiber laser acoustic sensor was presented. The DBR fiber laser acoustic sensor demonstrated the unique directional sensing abilities by means of beat frequency nonlinear modulation corresponding to the different acoustic propagation direction, and can measure the frequency, the power density and propagation directions of acoustic wave simultaneously by modulation signal analysis. Several DBR fiber lasers acoustic sensors could be multiplexed using existing optical fiber technology and detected by relative simple RF instruments, offering a great potential for the future application in optical fiber vector acoustic sensor systems.

Acknowledgments

This work was supported by Project of Natural Science Foundation of China (61205075), and Project of Tianjin Oceanic Administrator (KJZH2011-02).